iScience

CellPress
OPEN ACCESS

Article

An extended SARS-CoV-2 mRNA vaccine prime-boost interval enhances B cell immunity with limited impact on T cells

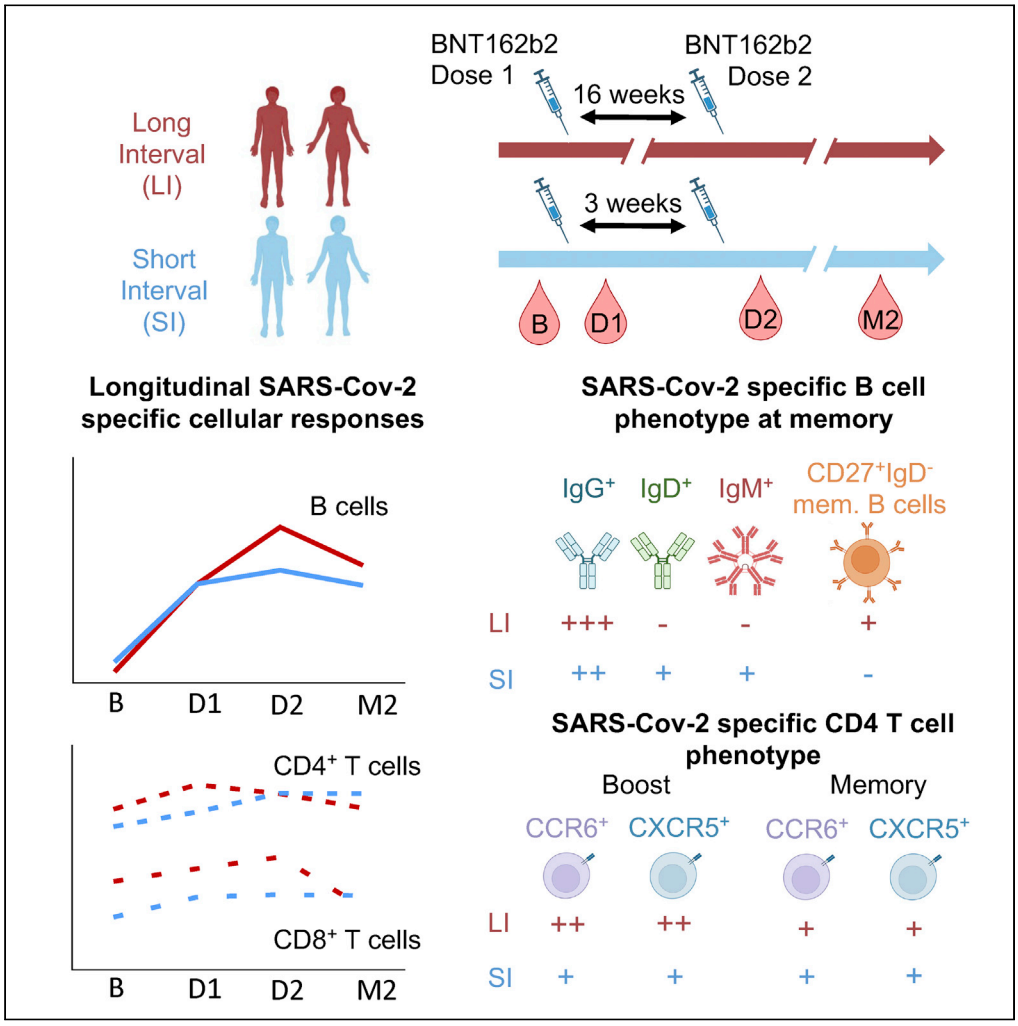

Alexandre Nicolas, Gérémy Sannier, Mathieu Dubé, ..., Allison R. Greenplate, E. John Wherry, Daniel E. Kaufmann

daniel.kaufmann@chuv.ch

Highlights

A 16-week interval increases B cell response and maturity compared to a 3-week delay

A 16-week interval has limited impact on the magnitude of CD4 and CD8 T cell responses

A long interval is associated with an early increase of specific SARS-CoV-2 cTfh

T cell phenotypes in 16-week versus 3-week regimens converge at late time points

Nicolas et al., iScience 26, 105904
January 20, 2023
https://doi.org/10.1016/j.isci.2022.105904

iScience

CellPress
OPEN ACCESS

Article

An extended SARS-CoV-2 mRNA vaccine prime-boost interval enhances B cell immunity with limited impact on T cells

Alexandre Nicolas,[1,2,9] Gérémy Sannier,[1,2,9] Mathieu Dubé,[1] Manon Nayrac,[1,2] Alexandra Tauzin,[1,2] Mark M. Painter,[3,4,5] Rishi R. Goel,[3,4] Mélanie Laporte,[1] Gabrielle Gendron-Lepage,[1] Halima Medjahed,[1] Justine C. Williams,[5] Nathalie Brassard,[1] Julia Niessl,[1,2,8] Laurie Gokool,[1] Chantal Morrisseau,[1] Pascale Arlotto,[1] Cécile Tremblay,[1,2] Valérie Martel-Laferrière,[1,2] Andrés Finzi,[1,2] Allison R. Greenplate,[3,4] E. John Wherry,[3,4,5] and Daniel E. Kaufmann[1,6,7,10,*]

SUMMARY

Spacing the first two doses of SARS-CoV-2 mRNA vaccines beyond 3–4 weeks raised initial concerns about vaccine efficacy. While studies have since shown that long-interval regimens induce robust antibody responses, their impact on B and T cell immunity is poorly known. Here, we compare SARS-CoV-2 naive donors B and T cell responses to two mRNA vaccine doses administered 3–4 versus 16 weeks apart. After boost, the longer interval results in a higher magnitude and a more mature phenotype of RBD-specific B cells. While the two geographically distinct cohorts present quantitative and qualitative differences in T cell responses at baseline and after priming, the second dose led to convergent features with overall similar magnitude, phenotype, and function of $CD4^+$ and $CD8^+$ T cell responses at post-boost memory time points. Therefore, compared to standard regimens, a 16-week interval has a favorable impact on the B cell compartment but minimally affects T cell immunity.

INTRODUCTION

The standard SARS-CoV-2 mRNA vaccine regimens recommend an interval of 21 days (Pfizer-BioNTech BNT162b2) or 28 days (Moderna mRNA-1273) between vaccine doses. However, the optimal interval has not been determined in controlled trials. In the context of vaccine scarcity and given the significant protection already conferred by the first dose in non-high-risk populations,[1–3] some public health agencies implemented schedules with longer intervals to rapidly extend population coverage.[4–6] While such strategies generated concerns given uncertain immunogenicity, a longer period of partial vulnerability to infection, and a hypothetical risk of escape mutant selection, epidemiological evidence supports this approach as a valid alternative in lower-risk populations[7,8] in which robust T cell and antibody responses are observed after a single dose.[9] Recent reports suggest that an extended interval between priming and boost procured enhanced humoral responses.[10–13]

As protective antibodies are associated with vaccine efficacy,[14,15] there is a need to better understand the generation and maintenance of B cell memory responses elicited by different vaccine modalities. As $CD4^+$ T cell help provided by T follicular helper (Tfh) is critical for the expansion, affinity maturation, and memory development of B cells,[16–19] it is also important to determine whether dosing interval affects $CD4^+$ and $CD8^+$ T cell vaccine responses. Demonstrating a direct protective role of SARS-CoV-2-specific $CD4^+$ and $CD8^+$ T cells independent of humoral immunity has been more challenging, but a number of studies support the notion that these lymphocyte subsets may contribute to recovery from COVID-19: Th1 cells, which foster development of $CD8^+$ T cell memory,[20] and Th17 are important for mucosal immunity.[21] However, T cell subsets show important heterogeneity and plasticity, better fitting with spectra of phenotypes and functions than fully distinct populations.[22] Previous studies by our group[21] and others[23,24] have demonstrated that SARS-CoV-2-specific $CD4^+$ T cells generated after the first vaccine dose predicted the humoral, B cell and $CD8^+$ T cell responses at later time points.

[1]Centre de Recherche du CHUM, Montréal, QC H2X 0A9 Canada

[2]Département de Microbiologie, Infectiologie et Immunologie, Université de Montréal, Montréal, QC H2X 0A9, Canada

[3]Institute for Immunology, University of Pennsylvania Perelman School of Medicine, Philadelphia, PA 19104, USA

[4]Immune Health®, University of Pennsylvania Perelman School of Medicine, Philadelphia, PA 19104, USA

[5]Department of Systems Pharmacology and Translational Therapeutics, University of Pennsylvania, Philadelphia, PA 19104, USA

[6]Département de Médecine, Université de Montréal, Montréal, QC H3T 1J4, Canada

[7]Division of Infectious Diseases, Department of Medicine, University Hospital of Lausanne and University of Lausanne, Lausanne, Switzerland

[8]Present address: Center for Infectious Medicine, Department of Medicine Huddinge, Karolinska Institutet, Stockholm, 171 77, Sweden

[9]These authors contributed equally

[10]Lead contact

*Correspondence: daniel.kaufmann@chuv.ch

https://doi.org/10.1016/j.isci.2022.105904

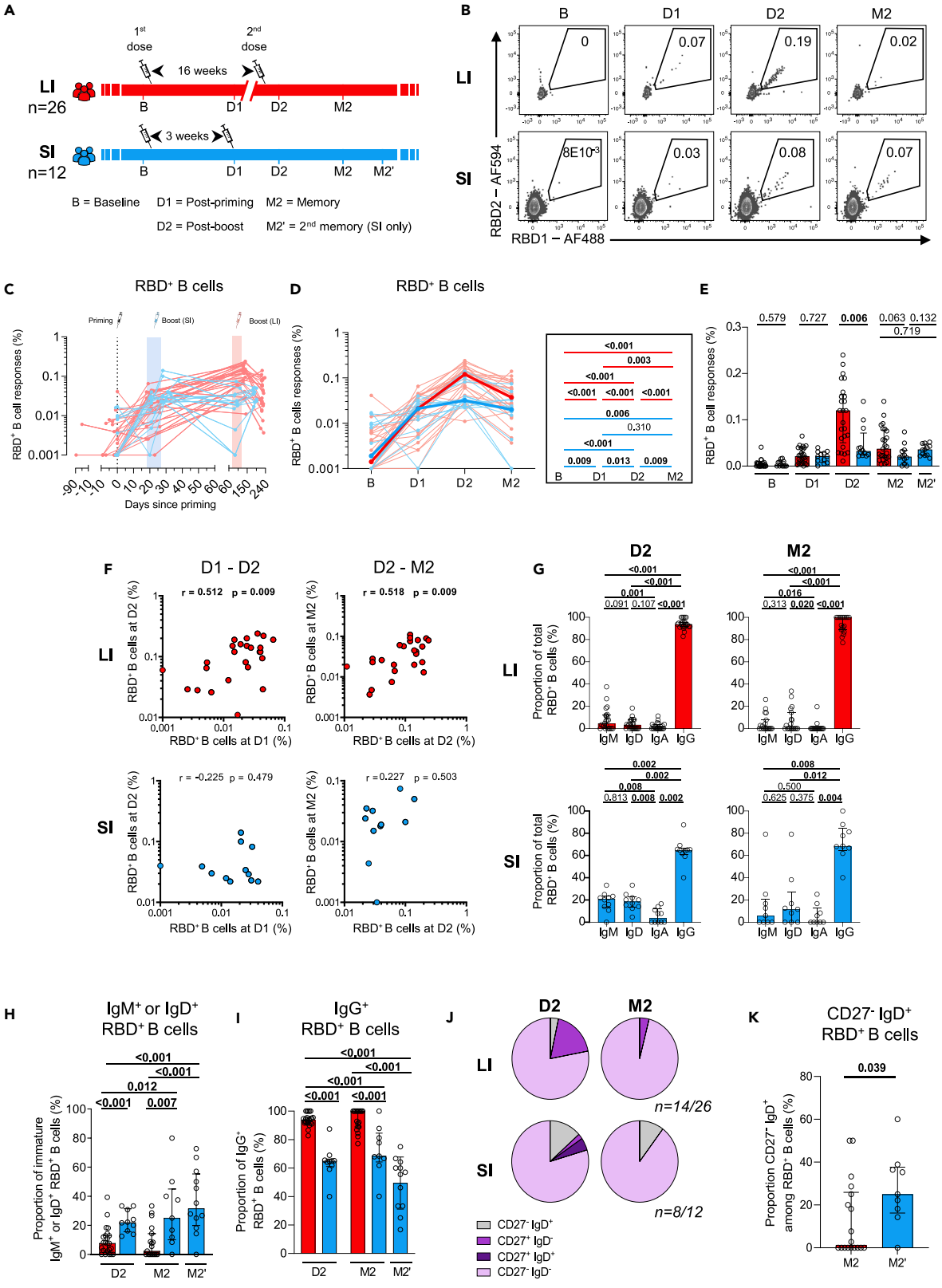
A
1st dose
2nd dose
16 weeks
LI
n=26
B
D1
D2
M2
3 weeks
SI
n=12
M2'
B = Baseline
D1 = Post-priming
M2 = Memory
D2 = Post-boost
M2' = 2nd memory (SI only)
B
D1
D2
M2
LI
SI
0
0.07
0.19
0.02
8E10-3
0.03
0.08
0.07
RBD2 – AF594
RBD1 – AF488
C
RBD+ B cells
Priming
Boost (SI)
Boost (LI)
RBD+ B cell responses (%)
Days since priming
D
RBD+ B cells
RBD+ B cells responses (%)
<0.001
0.003
<0.001
<0.001
<0.001
<0.001
0.006
0.310
<0.001
0.009
0.013
0.009
E
RBD+ B cell responses (%)
0.579
0.727
0.006
0.063
0.132
0.719
F
D1 - D2
D2 - M2
r = 0.512 p = 0.009
r = 0.518 p = 0.009
r = -0.225 p = 0.479
r =0.227 p = 0.503
RBD+ B cells at D1 (%)
RBD+ B cells at D2 (%)
RBD+ B cells at M2 (%)
G
D2
M2
Proportion of total RBD+ B cells (%)
IgM IgD IgA IgG
H
IgM+ or IgD+ RBD+ B cells
Proportion of immature IgM+ or IgD+ RBD+ B cells (%)
I
IgG+ RBD+ B cells
Proportion of IgG+ RBD+ B cells (%)
J
D2
M2
n=14/26
n=8/12
CD27- IgD+
CD27+ IgD-
CD27+ IgD+
CD27- IgD-
K
CD27- IgD+ RBD+ B cells
0.039
Proportion CD27- IgD+ among RBD+ B cells (%)

Figure 1. A 16-week delayed boost enhances the magnitude and maturation of B cell responses

(A) Schematic representation of study design. Blood samples were analyzed at four-time points in the long (red) interval (LI) and short (blue) interval (SI) cohorts: baseline (B); 3 weeks after priming (D1), 1–3 weeks after boost (D2), and 10–16 weeks after boost (M2). For SI participants, a later M2′ time point (23 weeks after boost) was also analyzed.

(B) Representative examples of RBD-specific B cell responses.

(C–E) Kinetics of RBD-specific B cell responses in LI (red) vs SI (blue) cohorts.

(C) Individual responses according to time of sampling. Colored background and syringe indicate the time of dose injections. Dots indicate time points examined.

(D) The bold line represents cohort's median value. Right panel: Wilcoxon tests.

(E) Inter-cohort comparisons. Bars represent medians ± interquartile ranges. Mann-Whitney tests are shown.

(F) Scatterplots showing temporal RBD^+ B cell correlations in the LI and SI cohorts. r: correlation coefficient. Significant correlations by Spearman tests ($p < 0.05$) are shown in bold.

(G) Frequencies of IgD, IgM, IgA, and IgG-positive cells within RBD-specific B cells within each cohort. Bars represent medians ± interquartile ranges. Paired comparisons were performed with Wilcoxon tests.

(H) Proportion of IgM^+ and IgD^+ ORgate cells among RBD^+ B cell cells. Bars represent medians ± interquartile ranges with Mann-Whitney tests for comparisons between the LI and SI cohorts.

(I) Proportion of IgG+ cells within RBD-specific B cells. Bars represent medians ± interquartile ranges, with Mann-Whitney tests for comparisons between the LI and SI cohorts.

(J) Proportion of $IgD^{+/-}$ and $CD27^{+/-}$ populations in RBD-specific B cells.

(K) Comparison of CD27-IgD + cells within RBD-specific B cells between the LI and SI cohorts. Bars represent medians ± interquartile ranges, Mann-Whitney tests are shown. In (C–F) n = 26 for long-interval (LI), n = 12 short-interval (SI). In (G, H, I, and K), n = 19 long-interval (LI), n = 9 short interval (SI). In (J), only the D2 and M2 time points provided enough events for analysis. n = 14 for long-interval (LI), n = 8 short-interval (SI). In (F–J), phenotypic analyses include samples for which more than 5 RBD^+ B cells were measured.

However, in contrast to the important progress made in the understanding of the kinetics of B and T cell responses in short-interval mRNA vaccine schedules,[23–26] how a long interval between the first two vaccine doses affects B and T cell immunity compared to standard dosing regimens remains poorly known due to the paucity of studies performing side-by-side comparisons with the same cellular immunity assays.[10,12,27]

Here, we apply standardized high-parameter flow cytometry assays to longitudinally compare the quantitative and qualitative features of vaccine-induced Spike-specific B cells, $CD4^+$ T cells, and $CD8^+$ T cells in SARS-CoV-2 naive participants enrolled in two cohorts: participants who received the two mRNA vaccine doses administered 16 weeks apart, defined as a long interval regimen; and participants who received the two doses 3-4 weeks apart, defined as a short-interval regimen.

RESULTS

Study participants

We evaluated immune responses in two independent cohorts of health care workers (HCW) that received two doses of mRNA vaccines (Figure 1A). The two cohorts differed by the time interval between the priming and the boosting inoculations, which defined the long interval (LI) cohort (16-week spacing, n = 26; Montreal cohort) and the short-interval (SI) cohort (3-4 weeks spacing, n = 12; Philadelphia cohort). Blood samples were examined at baseline (B) before vaccination; 3 weeks after the first dose (D1); 1-3 weeks after the second dose (D2), and 10 to 16 weeks after the second dose (M2). A later M2′ time point (median 23 weeks (22-25) after the second dose) was also analyzed in SI participants to provide a better comparison to M2 from LI volunteers. Clinical characteristics are shown in Table 1. The median age of the participants in the short-interval cohort was 15-year-old significantly younger (Mann-Whitney p = 0.019). Both cohorts significantly differed in the interval between prime and boost, and in the time of sampling D2 (3 weeks post second dose for LI, 1 week for SI) and M2 (16 weeks post second dose for LI, 10 for SI). No other statistical differences were noted.

A 16-week delayed boost enhances the magnitude and maturation of B cell responses

To evaluate SARS-CoV-2-specific B cells, we focused on the Receptor Binding Domain (RBD) of Spike to minimize the inclusion of B cells cross-reactive to endemic coronaviruses.[28,29] Co-detection of two fluorescently labeled recombinant RBD probes greatly enhances specificity (Figure 1B and[30] flow cytometry panel, Table S1; gating strategy, Figure S1A). We examined the magnitude of RBD-specific B cells (defined as $RBD1^+RBD2^+CD19^+CD20^+$) in the two cohorts (Figure 1C). Most participants showed no signal at baseline, and clear RBD-specific B cell responses after priming that were very similar between the LI and SI cohorts at the D1 time point, as expected. In the LI cohort, the second dose elicited robust recall responses at D2, followed by a decline at M2. The recall response in SI participants was more modest and plateaued at

Table 1. Clinical characteristics of the study participants[a]

	Long Interval (LI)[b]	Short Interval (SI)[b]
Prime-boost interval[c]	16 weeks apart	3 weeks apart
Variable[c]	(n = 26)	(n = 12)
Vaccine regimen		
Pfizer BNT162b2 vaccine (2 doses)	n = 25	n = 11
Heterologous vaccine strategy (Moderna mRNA-1273 and Pfizer BNT162b2)	n = 1	n = 0
Moderna mRNA-1273 vaccine (2 doses)	N = 0	n = 1
Age (years)[c]	51 (41–56)	38 (22–63)
Sex		
Male	11 (42%)	4 (33%)
Female	15 (58%)	8 (66%)
Vaccine dose spacing (days)		
Days between doses 1 and 2[c]	111 (109–112)	21 (20–28)
Visits for immunological profiling (days)		
B, days before first dose	1 (0–5)	0 (-1–1)
D1, days after first dose	21 (19–26)	21 (20–28)
D1, days before second dose	90 (85–92)	0 (-1–0)
D2, days after first dose[c]	133 (130–139)	29 (27–38)
D2, days after second dose[c]	21 (20–27)	7 (7–12)
M2, days after first dose	224 (222–228)	94 (86–115)
M2, days after second dose[c]	112 (110–119)	70 (65–94)
M2′, days after first dose		186 (196–181)
M2′, days after second dose		165 (175–153)

[a]Values displayed are medians, with IQR: interquartile range in parentheses for continuous variables, or percentages for categorical variables.
[b]The Long-interval (LI) and Short-interval (SI) cohorts were compared by the following statistical tests: for continuous variables, Mann-Whitney test, for categorical variables, Fisher's test.
[c]Statistically different values between the LI and SI cohorts ($p < 0.05$).

M2 and M2′ (Figures 1C–1E). The LI individuals globally peaked at higher magnitudes of RBD^+ B cell responses despite being globally older (Figure 1E) but converged with the SI cohort at subsequent memory time points (Figures 1C–1E). In contrast to short-interval participants, where no temporal association could be found between post-prime RBD^+ B cell responses and post-boost RBD^+ B cells, a strong and statistically significant positive correlation was observed in the long-interval cohort (Figure 1F). Likewise, RBD^+ B cell responses at D2 were associated with stronger memory responses in the long-interval cohort (Figure 1F).

We next determined whether the interval between vaccine doses qualitatively impacted the development of antigen-specific B cells by measuring IgM, IgD, IgA, and IgG expression on RBD-specific B cells (Figure S1B). To avoid excessive noise in phenotyping analyses, we only included donors in whom we detected $\geq$5 RBD-specific B cells at every time point. RBD-specific B cells from LI and SI donors were dominated by IgG^+ at both D2 and M2 time points (Figures 1G and S1C). However, a higher proportion of unswitched IgM^+ or IgD^+ RBD-specific B cells was detected at both time points in the SI cohort (Figures 1H and S1D). Consequently, the proportion of IgG^+ RBD^+ B cells was lower in the SI than in the LI cohort (Figure 1I). Both the elevated proportion of immature IgM^+/IgD^+ RBD-specific B cells (Figure S1E) and decreased proportion of IgG^+ RBD-specific B cells were observed at the later M2′ SI time point (Figure S1F). Thus, when comparing M2′ SI with M2 LI, additional maturation time did not mitigate the differences in IgM^+/IgD^+ and IgG^+ RBD-specific B cells proportion between both cohorts (Figures 1H and 1I).

To assess RBD-specific B cell differentiation, we next quantified IgD and CD27 co-expression (Figure S1G). CD27 is predominantly expressed on memory B cells,[31] and IgD on unswitched B cells.[32] An atypical double-negative (DN) IgD^-CD27^- was dominant at both the D2 and M2 time points in both cohorts (Figures 1J

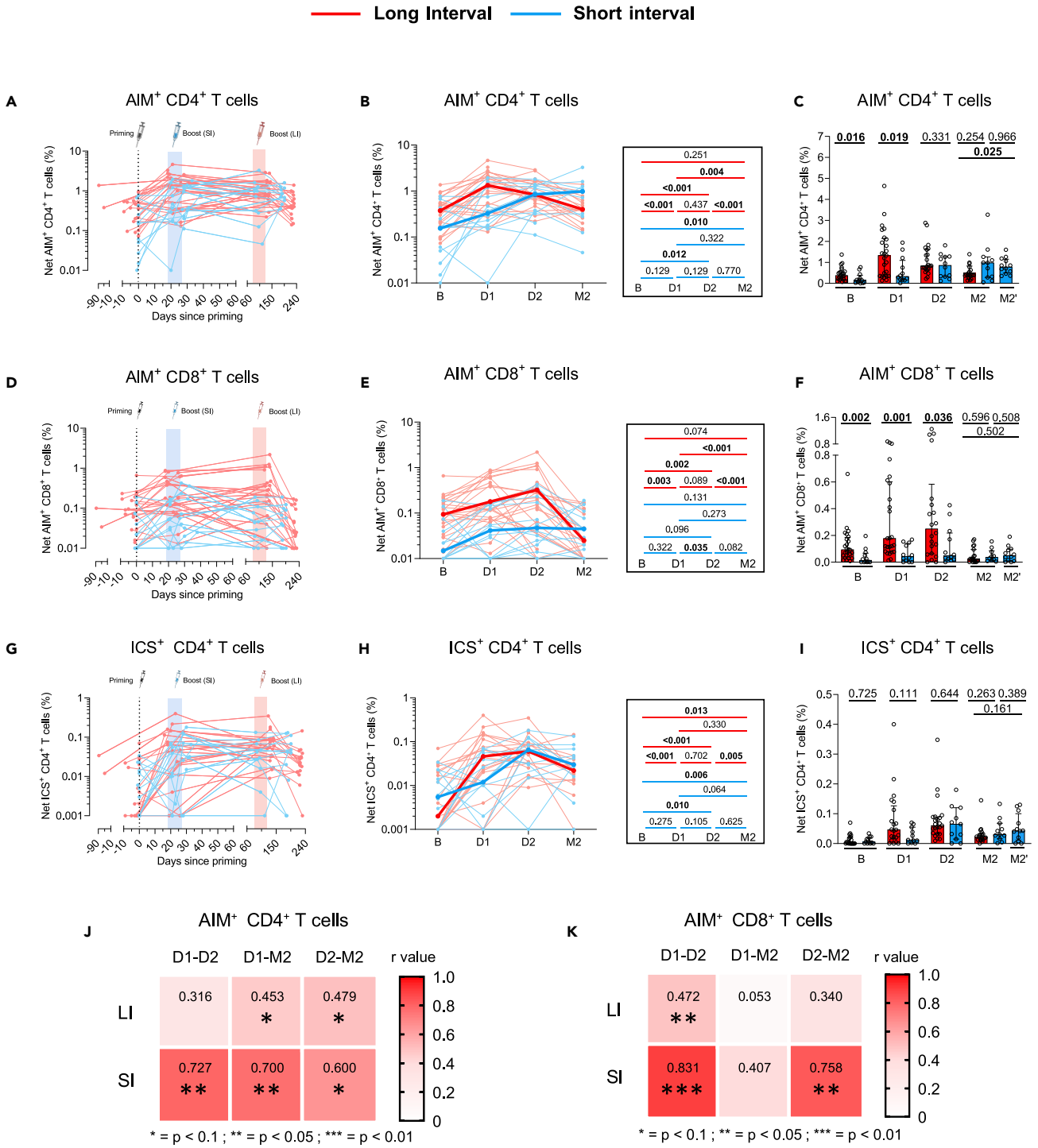

Figure 2. The initial two-dose vaccination series elicits Spike-specific CD4+ T cell responses of similar magnitude irrespective of dosing interval

SARS-CoV-2 Spike-specific CD4+ and CD8+ T cells in long (red) and short (blue) receiving two vaccine doses.

(A–C) Longitudinal (A and B) and inter-cohort (C) analyses of net Spike-specific AIM+ CD4+ T cell responses.

(D–F) Longitudinal (D and E) and inter-cohort (F) analyses net AIM+ CD8+ T cell responses.

Figure 2. *Continued*

(G–I) Longitudinal (G and H) and inter-cohort (I) analyses of the net magnitude of cytokine$^+$ CD4$^+$ T cell responses. The bold lines in B, E and H represent median values. The bars in C, F and I represent median ± interquartile ranges. In (B, E, H), the right panel shows statistical comparisons using Wilcoxon tests. In (C, F, I), Mann-Whitney tests are shown for inter-cohort comparisons and Wilcoxon tests for intra-cohort comparisons.

(J and K) Heatmap showing temporal correlations of (J) AIM$^+$ CD4$^+$ and (K) AIM$^+$ CD8$^+$ T cells between the different time points for the two cohorts. The numbers in high square represent the correlation coefficient r. Significant Spearman tests results are indicated by stars (*: $p < 0.1$, **: $p < 0.05$, ***: $p < 0.001$). In A-K) LI cohort: n = 26, SI cohort: n = 12.

and S1H). In the LI cohort, class-switched memory IgD$^-$CD27$^+$ RBD-specific B cells were present at D2 and subsequently contracted at M2. This more mature subset was negligible at both time points in the SI cohort. Immature IgD$^+$CD27$^-$ were rarely observed in LI participants, contrasting with their sizable proportion at M2 and M2′ in the SI cohort (Figures 1J and S1I). There was a trend for a higher proportion of unswitched RBD-specific B cells in SI compared to LI at M2. This difference reached significance when comparing LI M2 with SI M2′, time points that are more comparable (Figure 1K).

The SI and LI cohorts studied here represent subsets of cohorts in which we previously studied humoral responses in-depth.[13] To contextualize our RBD-specific B cells analysis, we plotted the humoral responses against RBD in our cohorts (Figure S1J). We observed no statistically significant differences in the magnitude of RBD-specific antibody responses between the LI and SI cohorts at corresponding time points (Figures S1K and S1L). However, we observed a significantly higher RBD avidity at M2 in the LI cohort (Figure S1M), in agreement with a previous report showing higher RBD avidity in individuals receiving a long interval compared to a short interval.[13]

These data show that compared to the standard short-interval regimen, the second vaccine dose given after a long 16-week interval elicited robust RBD$^+$ B cell responses peaking at higher magnitude than a shorter 3-week interval. The longer interval resulted in increased B cell maturity and stronger associations between early post-boost and memory responses.

The initial two-dose vaccination series elicits spike-specific CD4$^+$ T cell responses of similar magnitude irrespective of dosing interval

CD4$^+$ T cells help play a critical role in the development of B cell and CD8$^+$ T cell immunity. We, therefore, measured Spike-specific T-cell responses at the four time points in the two cohorts (Figures 2 and S2). As in our previous work,[9] we used both a TCR-dependent activation-induced marker (AIM) assay that broadly identifies antigen-specific T cells and intracellular cytokine staining (ICS) to perform functional profiling (flow cytometry panels: Tables S2 and S3).

The AIM assay involved a 15-h incubation of PBMCs with an overlapping peptide pool spanning the Spike coding sequence of the ancestral strain and the measurement of CD69, CD40L, 4-1BB and OX40 upregulation upon stimulation. We used an AND/OR Boolean combination gating to assess the total frequencies of antigen-specific CD4$^+$ and CD8$^+$ T cells (Figures S2A and S2B).[9,33] At D2, all individuals had detectable CD4$^+$ T cell responses (Figure S2C), and most had measurable CD8$^+$ T cell responses (Figure S2D).

AIM CD4$^+$ T cell responses in the two cohorts differed at baseline and after the first dose (Figure 2A). An increased plasma antibody binding to the prevalent OC43 betacoronavirus was noted in the LI cohort (Figure S2E). It raises the possibility that the higher AIM responses at baseline of LI are the consequences of previous cross-reactive expositions to common coronaviruses,[34,35] although pre-exposition to abortive infection without seroconversion is also possible.[36] The effect of the second dose in LI was modest, with AIM CD4$^+$ T cell responses still higher than at baseline, but lower than the initial responses at D1. In contrast, in SI the second dose further increased after an initially weaker CD4$^+$ T cell response. Despite these initial differences, the trajectories converged at D2 (Figures 2B and 2C). In LI participants, the AIM CD4$^+$ T cell responses decreased at the memory time points, a decline not yet observed in the SI cohort owing to a comparatively earlier sampling.

The trajectories of AIM$^+$ CD8$^+$ T responses were heterogeneous (Figure 2D). As reported in our previous study,[21] LI participants elicited weak but significant responses after priming, a trend for stronger responses after the boost and contraction at M2 (Figure 2E). Consistent with AIM$^+$ CD4$^+$ T cell responses, AIM$^+$ CD8$^+$ T cell responses in the SI cohort were lower at baseline and D1 (Figure 2F). AIM$^+$ CD8$^+$ T responses

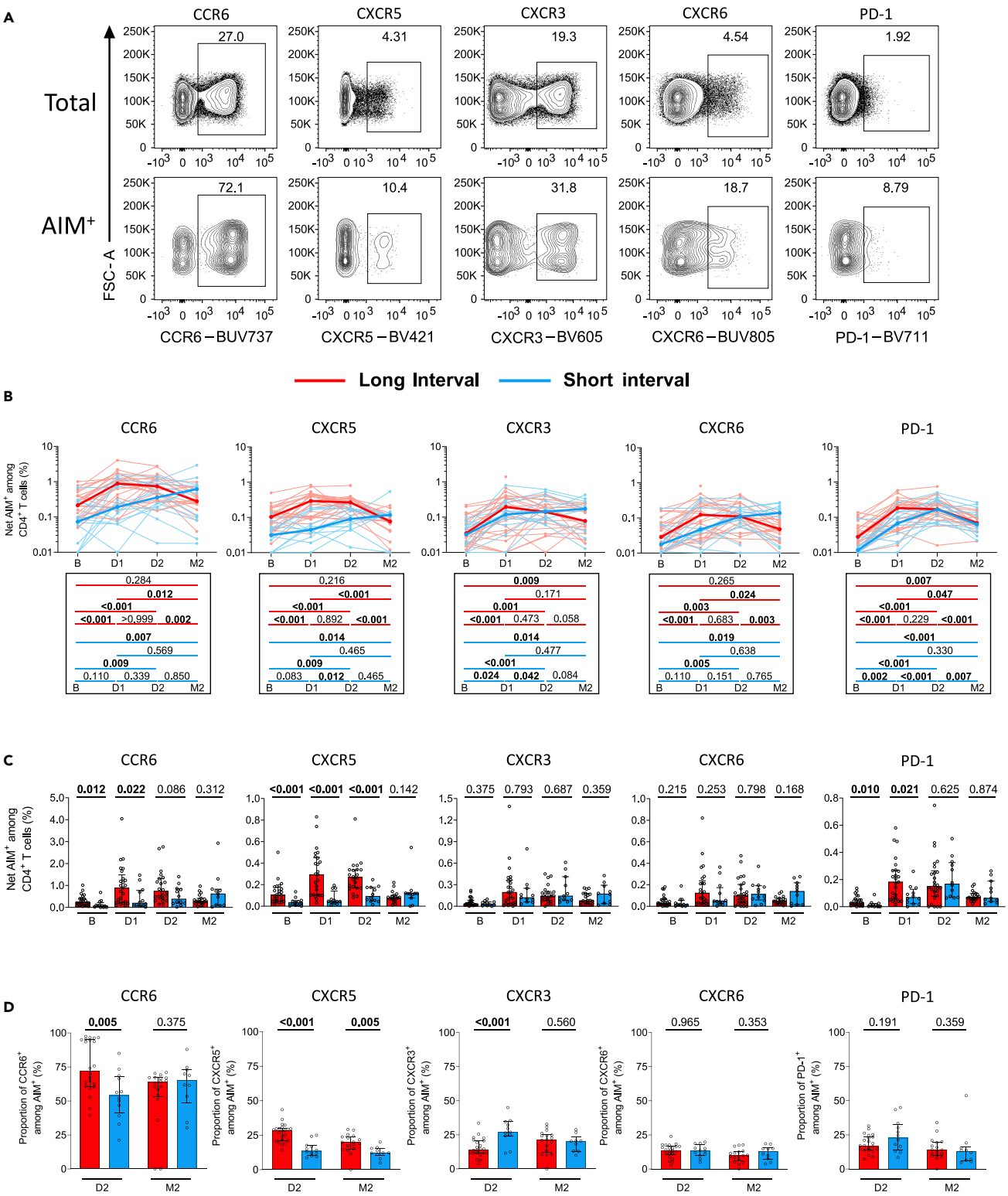

Figure 3. The second dose leads to convergence of some CD4$^+$ T helper differentiation features differing early between the LI and SI cohorts

(A) Representative flow cytometry dot plots for the indicated univariate phenotypic populations.

(B) Net longitudinal frequencies of each AIM$^+$ CD4$^+$ T cell subpopulation in LI (red) and SI (blue) cohorts. Bold lines represent cohort's median value. Bottom panel: Wilcoxon tests for each pairwise comparison.

Figure 3. *Continued*

(C) Cohort comparisons at each time point for the subsets presented in (A). The bars represent median ± interquartile ranges. Mann-Whitney tests are shown.

(D) Proportion of CXCR5$^+$, CXCR3$^+$, CCR6$^+$, CXCR6$^+$ and PD-1$^+$ cells in total AIM$^+$ CD4$^+$ T cells at the D2 and M2 time points following the second dose. Bars represent medians ± interquartile ranges. Mann-Whitney tests are shown.

(B–D) Phenotypic analyses include only individuals for which the spike-specific signal was ≥2 times over the background, with ≥5 positive events. (BCD) LI cohort: n = 26, SI cohort: n = 12.

plateaued from D2 up to M2′ at levels comparable to the post-attrition levels seen in the LI cohort (Figures 2E and 2F), again indicating a convergence between the two vaccine modalities.

The ICS assay involved a 6-h stimulation with the Spike peptide pool and measurement of the effector molecules IFN-γ, IL-2, TNF-α, IL-17A, IL-10, and CD107a. We defined cytokine$^+$CD4$^+$ T cell responses by an AND/OR Boolean gating strategy (Figure S2F). Cytokine$^+$ CD4$^+$ T effector cells were readily detected after vaccination in most participants (Figure S2G). Total cytokine$^+$ CD8$^+$ T cell responses were weak or undetectable in most participants, precluding their detailed analysis (Figure S2H). The ICS patterns in both cohorts paralleled the AIM assays, albeit at a lower magnitude (Figure 2G). Cytokine responses in SI and LI converged at D2 and remained similar at M2 and M2′ (Figures 2H and 2I). In contrast to AIM, however, cytokine$^+$ CD4$^+$ T cell responses at M2 remained significantly higher than at baseline in both cohorts (Figure 2H), showing longer-term memory poised for exerting effector functions.

As the expansion of previously primed antigen-specific T cells may impact T cell responses to vaccination, we examined correlations across visits (Figures 2J and 2K). We found in the LI cohort weak associations between post-priming AIM$^+$ CD4$^+$ T cell responses and those measured after boost or at the memory time point, respectively (Figure 2J). These associations were stronger in SI participants. We also found temporal associations for Spike-specific CD8$^+$ T responses despite their lower magnitudes (Figure 2K).

These data show that in contrast to B cell responses, the initial differences in the magnitude of Spike-specific CD4$^+$ and CD8$^+$ T cell responses that we observed between cohorts prior and early after priming disappeared after the second dose. The similar responses at the memory time point suggest that the time interval between the two doses has a limited impact on the emergence and maintenance of Spike-specific CD4$^+$ and CD8$^+$ T cell immunity.

The second dose leads to convergence of some CD4$^+$ T helper differentiation features differing early between the LI and SI cohorts

As the interval had a limited impact on the generation of CD4$^+$ T cells but B cell responses remained lower after the second dose, we tested if different intervals could qualitatively affect CD4$^+$ T cell responses and compared key CD4$^+$ T cell subsets at D2 and M2 (Figure 3). We examined chemokine receptors that are preferentially, but not exclusively, expressed by some lineages and are involved in tissue homing (CXCR5 for Tfh; CXCR3 for Th1; CCR6 for Th17 and Th22 and mucosal homing; CXCR6 for pulmonary mucosal homing,[37,38] and PD-1 as an inhibitory checkpoint (Figure 3A)), and assessed their longitudinal fluctuations (Figures 3B and 3C).

CCR6$^+$ cells were dominant in both cohorts, representing a median of 72% in LI and 54% in SI of all D2 responses, but with a wide inter-individual variation (Figure 3D). Median CXCR5$^+$ was 28% (LI) and 14% (SI), median CXCR3$^+$ was 14% (LI) and 27% (SI), and PD-1$^+$ was 17% (LI) and 23% (SI). CXCR6$^+$ cells were the rarest tested polarization, representing 13% (LI) and 14% (SI) of AIM$^+$ CD4$^+$ T cells. We observed a variable contribution of these Thelper subsets to the differences in total magnitude of CD4$^+$ T cell responses between the LI and SI cohorts at baseline and after priming (Figures 3B and 3C). The CCR6$^+$ and CXCR5$^+$ subset showed major differences, with increased frequencies in LI at D2, then convergence at M2, whereas the kinetics of the CXCR3$^+$ and CXCR6$^+$ subsets showed no significant differences at any time points in the two cohorts (Figures 3B and 3C). The PD-1$^+$ subset differed initially but exhibited similar magnitudes after the second dose and at M2 (Figures 3B and 3C). As shown by the relative fraction of each subset in the total AIM$^+$ CD4$^+$ T cell populations, some qualitative differences were still present shortly after the second dose but mostly waned at the memory time point (Figure 3D).

These results show that although the LI and SI cohorts presented qualitative differences at baseline and after the priming dose, repeat inoculation led to mostly converging features at the memory time point after the second dose despite the interval difference between doses in the two cohorts.

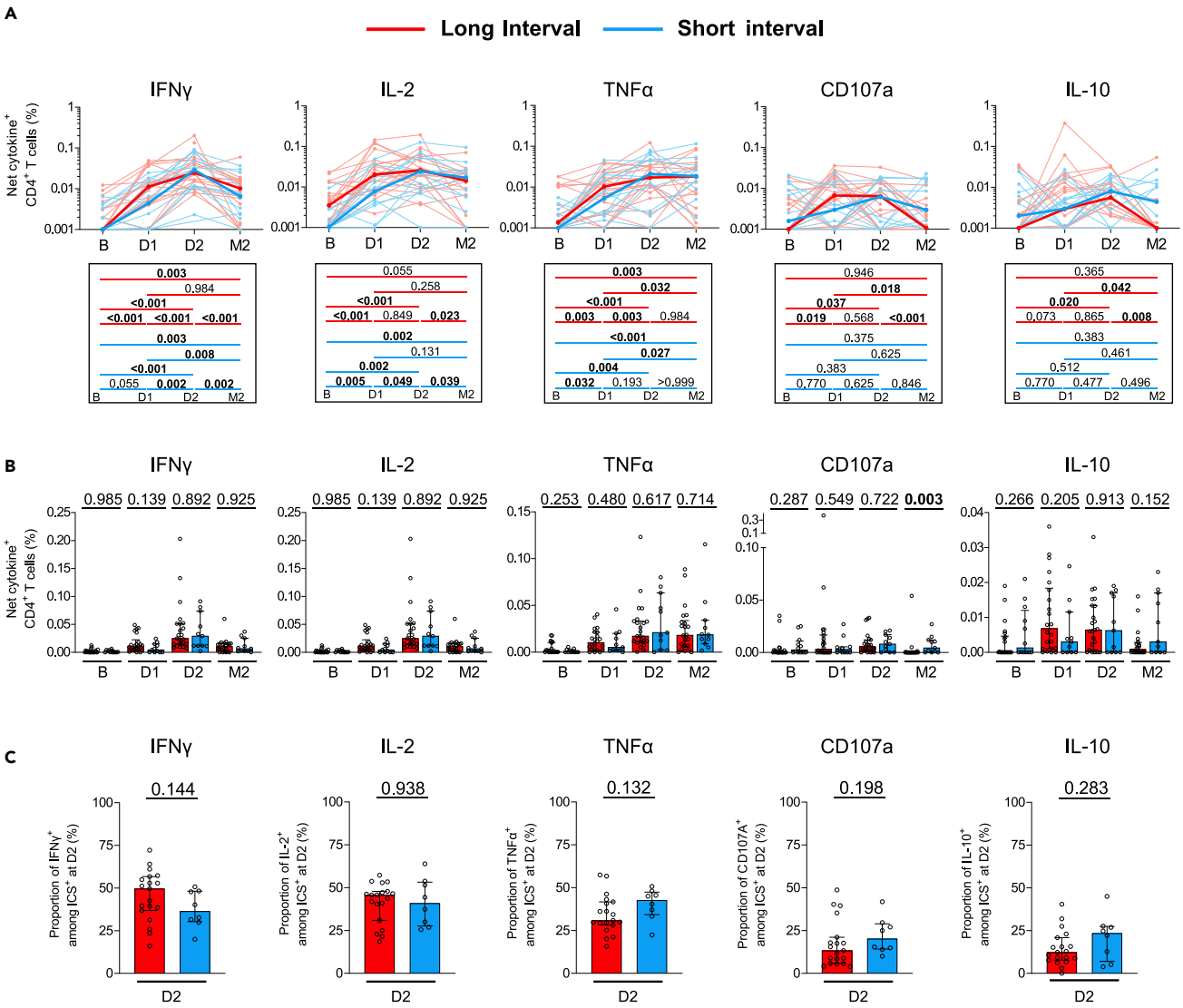

Figure 4. The long and short vaccination regimens elicit largely similar patterns of CD4⁺ T cell effector functions

(A) Longitudinal net frequencies of indicated cytokine⁺ CD4⁺ T cell subpopulations in the LI (red) and SI (blue) cohorts. Bold lines represent cohort's median value. Lower panel: Wilcoxon tests for each pairwise comparison.

(B) Cohort comparisons at each time point for each function represented in (A). The bars represent medians ± interquartile ranges. Mann-Whitney tests are shown.

(C) Proportions of IFN-γ, Il-2, TNF-α, IL-10, and CD107a-expressing cells among total cytokine⁺ CD4⁺ T cells. Bars represent medians ± interquartile ranges. Mann-Whitney tests are shown to compare long and short-interval cohorts.

(A-C) Phenotypic analyses include only individuals for which the spike-specific signal was ≥2 times over the background, with ≥5 positive events. (AB) LI cohort: n = 26, SI cohort: n = 12. (C) LI cohort: n = 19, SI cohort: n = 8.

The long and short vaccination regimens elicit largely similar patterns of CD4⁺ T cell effector functions

We next compared effector functions by ICS at D2 and M2, focusing on IFN-γ, TNF-α, IL-2, IL-10, and CD107a (Figures 4A–4C). IFN-γ⁺ and IL-2⁺ CD4⁺ T cells contracted at M2 in both cohorts, whereas TNFα remained constant (Figures 4A and 4B). A decline of CD107a⁺ and IL-10⁺ CD4⁺ T cells was also observed at M2 in both cohorts, but was more pronounced in the LI, consistent with the later time of sampling. After the second dose, we did not detect any statistically significant differences in the qualitative functional profile of CD4⁺ T cell responses elicited by the long and short-interval vaccination schedules, as illustrated by the relative fraction of each cytokine in the total ICS response (Figure 4C).

Therefore, a longer interval between the first and second doses does not significantly alter the profile of tested effector $CD4^+$ T functions.

DISCUSSION

Several studies have shown that extending the interval between the first two doses of SARS-CoV-2 mRNA vaccines beyond the recommended regimens of 3-4 weeks can lead to stronger antibody responses.[10–13] These studies have led some public health agencies to modify their vaccination guidelines accordingly (eg., 8 weeks or more between the primary two doses in Quebec[39]). However, the impact of long-interval regimens on cellular immunity is still poorly known due to the paucity of studies performing side-by-side in-depth comparisons of different dosing regimens with the same assays. Here, we compared the antigen-specific B cell, $CD4^+$ T cell, and $CD8^+$ T cell responses elicited in SARS-CoV-2 naive participants by a 16-week interval regimen compared to the standard 3-4 weeks schedule. We observed that a long interval increased the magnitude and maturation of RBD-specific B cell responses, while the completion of the primary vaccine series led to quantitatively and qualitatively similar memory $CD4^+$ and $CD8^+$ T cell memory responses in both regimens.

The RBD-specific B cells responses to the first vaccine dose were very consistent between the two cohorts and did not appear impacted by the age difference between the groups. In contrast, the magnitude of these responses markedly differed after the second dose, with a robust increase in the LI cohort contrasting with a weak gain for the SI cohort. A second dose after a short interval might act like a prolonged antigen delivery rather than a recall of primed responses, thus explaining a more limited benefit. While the sampling time could contribute to differences observed early after the second dose, the differences persisted as a strong trend at M2 before a late convergence at M2′ memory time point. The increased B cell responses with a long interval are supporting recent findings showing that a longer interval also increases the peak humoral responses and antibody maturation,[10–12,40,41] and are consistent with the fact that germinal centers remain active for several weeks after vaccination,[42] with the continuous evolution of the B cell compartment for several months[43] and accumulation of somatic hypermutations.[18,42,44] Hence, an early second dose likely corresponds to a suboptimal timing in terms of re-exposure to the cognate antigen, while a longer interval allows for a better evolution of the B cell repertoire. In line with these findings, the B cell maturation profile differed between the LI and SI cohorts after the second dose: almost all RBD-specific B cells presented an isotype-switched IgG^+ phenotype in LI participants, contrasting with sizable IgM^+ and IgD^+ cell populations in SI volunteers which, importantly, persisted 23 weeks after boost. The memory differentiation phenotype was also consistent with this profile, with a larger fraction of RBD^+ B cells with a $CD27^+$ IgD^- memory phenotype early after boost in the LI participants. As we previously reported[21] the RBD-specific B cell responses were dominated by the double-negative $CD27^-$ IgD^- cells, including at the memory time point. This phenotypic subset was described in autoimmune diseases[45,46] and in response to vaccination.[47] $CD27^-$ IgD^+ RBD^+ B cells were absent at baseline and in previously infected individuals,[21] suggesting recently activated B cells. Taken together, these results suggest that the long-interval regimen is beneficial to the generation and maturation of the B cell compartment, consistent with the higher avidity achieved after the two doses of the long-interval schedule.

We observed that Spike-specific $CD4^+$ and $CD8^+$ T cell responses at baseline were significantly stronger in the LI compared to the SI cohort. While we cannot exclude that this difference is due to precedent abortive SARS-CoV-2 infection with no seroconversion,[36] other studies have shown that cross-reactive immunity to common coronaviruses plays a major role in shaping these pre-existing SARS-CoV-specific $CD4^+$ and $CD8^+$ T cell responses.[48–51] Of note, our two cohorts were of geographically distinct locations (LI: Montreal, SI: Philadelphia) and the LI participants were significantly older than the SI volunteers. While the lack of sufficient PBMC samples precluded direct testing of cross-reactivity for CD4 and CD8 T cell responses, the higher antibody recognition of the OC43 Spike by the plasma from the LI cohort supports the possibility that differential previous exposure to endemic coronaviruses contributes to the pre-vaccination differences observed. These differences persisted after the first vaccine dose, consistent with a previously reported association between pre-existing T cell immunity and responses after priming.[9,49,52,53] Importantly, however, the quantitative and qualitative differences in $CD4^+$ and $CD8^+$ T cell responses decreased already early after the second vaccine dose and waned almost entirely at the memory time point collected 10 to 16 weeks after the boost. This convergence was present both in phenotypic AIM assays (e.g, for $CXCR5^+$ and $CCR6^+$ $CD4^+$ T cells) and functional ICS assays. IFN- γ^+ and IL-2^+ $CD4^+$ T cell responses were

comparable in the two cohorts, consistent with a recent study.[10] Similarly, we did not identify differences in memory responses for TNF-α and IL-10 production. The small difference in $CD107a^+$ $CD4^+$ T cells frequencies should be interpreted with caution, given the very low magnitude of these responses. At first sight, our IL-2 data differ from another study that reported stronger memory $IL\text{-}2^+$ CD4 T cell responses in long-interval vaccination.[12] However, the timeline may contribute to these differences. In our study, we assessed memory later after the second dose (10-16 weeks versus 4 weeks in[12]). Therefore, the completion of the primary 2-dose vaccination leads to convergent $CD4^+$ and $CD8^+$ T cell memory responses irrespective of dosing interval.

While the initial rationale of delaying the second dose was to provide some level of immunity more rapidly to a larger number of people in the context of limited vaccine supply,[6] our results show that this strategy is beneficial to the generation of B cell responses without negative impact on T cell immunity. The potential immunological benefits of increasing the interval between doses must be weighed against a prolonged window of suboptimal protection, particularly while the virus and its different variants of concern are circulating in the population. Many countries now recommend a third dose, and more, although compliance with additional inoculations is a significant issue. Whether additional inoculations further abrogate the differences in cellular immunity observed between the long and short-interval regimens after the primary vaccination series warrants further investigation.

Limitations of the study

The cohorts were from two different countries that implemented different vaccination policies. As a result, the time points after the second dose were not perfectly matched. To mitigate this, we emphasized the direct comparisons on memory time points, which are less likely to be affected by the difference in the time of sampling.

The LI cohort is globally older than the SI cohort. Because age is associated with immune senescence,[54,55] we may underestimate the benefit of extending the delay between the two doses. Our global message remains that compared to the standard vaccination schedule, a longer interval provides equivalent or better spike-specific B, CD4, and CD8 T cell responses.

Here, we investigated individuals who were SARS-CoV-2 naive prior to vaccination. However, we did not investigate the impact of long versus short-interval vaccine regimens in previously infected people. Further comparative studies are therefore required to assess the impact of dosing interval on cellular hybrid immunity. Also, we could not measure the impact of pre-exposition to abortive SARS-CoV-2 infection.

The demographically distinct LI and SI cohorts presented differences in T cell responses at baseline that we interpreted as likely reflecting the presence of a pre-existing pool of cross-reactive cells to other coronaviruses. Formal demonstration would require epitope-specific mapping of T cell responses, for which we did not have enough PBMC samples available. Also, in the current study, we could not measure the impact of potential pre-exposition to abortive SARS-CoV-2 infection that might potentiate cellular responses in absence of seroconversion.

We analyzed the cellular responses to ancestral strain antigens corresponding to the mRNA vaccines. The limiting availability in PBMC did not allow to assess the impact of dosing interval on B and T cell responses to variants of concern.

The size of the cohorts investigated here, particularly of the short-interval group, is not sufficient to uncover potential smaller qualitative differences in the T cell responses that might be caused by different intervals. However, the contrasting results obtained for B cell responses compared to T cell responses are clear enough to conclude that modifying the time between vaccine inoculations has a much bigger impact on B cell than T cell immunity.

Our study conducted in a low-risk HCW cohort may not be generalizable to vulnerable groups, particularly immunocompromised or elderly populations, in which the cellular immune responses and the risk/benefit ratio may differ. Future studies will be required to better quantify the immune response over time in these populations.

STAR★METHODS

Detailed methods are provided in the online version of this paper and include the following:

SUPPLEMENTAL INFORMATION

Supplemental information can be found online at https://doi.org/10.1016/j.isci.2022.105904.

ACKNOWLEDGMENTS

The authors are grateful to the study participants. We thank the CRCHUM BSL3 and Flow Cytometry Platforms for technical assistance, Dr. Johanne Poudrier for advice and discussions. This work was supported by an FRQS Merit Research Scholar award to D.E.K, the Fondation du CHUM, the Ministère de l'Économie et de l'Innovation du Québec, Programme de soutien aux organismes de recherche et d'innovation (to A.F), a CIHR operating grant # 178344 (D.E.K and A.F), a foundation grant #352417 (A.F), a CIHR operating Pandemic and Health Emergencies Research grant #177958 (A.F), and an Exceptional Fund COVID-19 from the Canada Foundation for Innovation (CFI) #41027 to A.F and D.E.K. The Symphony flow cytometer was funded by a John R. Evans Leaders Fund Leader Fund from the Canada Foundation for Innovation (# 37521 to D.E.K) and the Fondation Sclérodermie Québec. A.F. is the recipient of Canada Research Chair on Retroviral Entry no. RCHS0235 950-232424. V.M.L. is supported by an FRQS Junior 1 salary award, G.S. is supported by an FRQS doctoral fellowship and by a scholarship from the Department of Microbiology, Infectious Disease, and Immunology of the University of Montreal. A.T. is supported by a Mitacs Accélération postdoctoral fellowship. This work was also supported by NIH funds: grants AI108545, AI155577, AI149680, and U19AI082630 (to E.J.W.), the University of Pennsylvania Perelman School of Medicine COVID Fund (to R.R.G. and E.J.W.); the University of Pennsylvania Perelman School of Medicine 21st Century Scholar Fund (to R.R.G.); and the Paul and Daisy Soros Fellowship for New Americans (to R.R.G). The funders had no role in study design, data collection and analysis, decision to publish, or preparation of the article. Some illustrations were created with Biorender.com.

AUTHOR CONTRIBUTIONS

A.N., G.S., M.D., A.F., and D.E.K. designed the studies. A.N., G.S., M.N., N.B., and M.L. performed B cell and T cell assays. A.N., G.S., and M.D. performed and analyzed the B and T cell experiments. G.G.L. and A.T. performed RBD ELISA, RBD avidity index and OC43 staining. J.N. contributed to the T cell assay design. A.T., H.M., L.G., C.M., P.A., C.T., J.C.W., and V.M.L. secured and processed blood samples. M.M.P., R.R.G., A.R.G., and E.J.W. provided unique reagents. G.G. produced and purified proteins. A.N., G.S., M.D., and D.E.K. wrote the article. Every author has read, edited, and approved the final article.

DECLARATION OF INTERESTS

A.R.G. is a consultant for Relation Therapeutics. E.J.W. is consulting for or is an advisor for Merck, Marengo, Janssen, Related Sciences, Synthekine, and Surface Oncology. E.J.W. is a founder of Surface Oncology, Danger Bio, and Arsenal Biosciences. The other authors have no conflict of interest to declare.

Received: August 8, 2022
Revised: November 10, 2022
Accepted: December 26, 2022
Published: January 20, 2023

REFERENCES

1. Baden, L.R., El Sahly, H.M., Essink, B., Kotloff, K., Frey, S., Novak, R., Diemert, D., Spector, S.A., Rouphael, N., Creech, C.B., et al. (2021). Efficacy and safety of the mRNA-1273 SARS-CoV-2 vaccine. N. Engl. J. Med. *384*, 403–416. https://doi.org/10.1056/NEJMoa2035389.

2. Skowronski, D.M., and De Serres, G. (2021). Safety and efficacy of the BNT162b2 mRNA Covid-19 vaccine. N. Engl. J. Med. *384*, 1576–1577. https://doi.org/10.1056/NEJMc2036242.

3. Polack, F.P., Thomas, S.J., Kitchin, N., Absalon, J., Gurtman, A., Lockhart, S., Perez, J.L., Pérez Marc, G., Moreira, E.D., Zerbini, C., et al. (2020). Safety and efficacy of the BNT162b2 mRNA Covid-19 vaccine. N. Engl. J. Med. *383*, 2603–2615. https://doi.org/10.1056/NEJMoa2034577.

4. Tuite, A.R., Zhu, L., Fisman, D.N., and Salomon, J.A. (2021). Alternative dose allocation strategies to increase benefits from constrained COVID-19 vaccine supply. Ann. Intern. Med. *174*, 570–572. https://doi.org/10.7326/M20-8137.

5. Paltiel, A.D., Zheng, A., and Schwartz, J.L. (2021). Speed versus efficacy: quantifying potential tradeoffs in COVID-19 vaccine deployment. Ann. Intern. Med. *174*, 568–570. https://doi.org/10.7326/M20-7866.

6. Rodrigues, C.M.C., and Plotkin, S.A. (2021). The influence of interval between doses on response to vaccines. Vaccine *39*, 7123–7127. https://doi.org/10.1016/j.vaccine.2021.10.050.

7. Carazo, S., Talbot, D., Boulianne, N., Brisson, M., Gilca, R., Deceuninck, G., Brousseau, N., Drolet, M., Ouakki, M., Sauvageau, C., et al. (2021). Single-dose mRNA vaccine effectiveness against SARS-CoV-2 in healthcare workers extending 16 weeks post-vaccination: a test-negative design from Quebec, Canada. Clin. Infect. Dis. *75*, e805–e813. https://doi.org/10.1093/cid/ciab739.

8. Skowronski, D.M., Setayeshgar, S., Febriani, Y., Ouakki, M., Zou, M., Talbot, D., Prystajecky, N., Tyson, J.R., Gilca, R., Brousseau, N., et al. (2021). Two-dose SARS-CoV-2 vaccine effectiveness with mixed schedules and extended dosing intervals: test-negative design studies from British Columbia and Quebec, Canada. Preprint at medRxiv. https://doi.org/10.1101/2021.10.26.21265397.

9. Tauzin, A., Nayrac, M., Benlarbi, M., Gong, S.Y., Gasser, R., Beaudoin-Bussières, G., Brassard, N., Laumaea, A., Vézina, D., Prévost, J., et al. (2021). A single dose of the SARS-CoV-2 vaccine BNT162b2 elicits Fc-mediated antibody effector functions and T cell responses. Cell Host Microbe *29*, 1137–1150.e6. https://doi.org/10.1016/j.chom.2021.06.001.

10. Hall, V.G., Ferreira, V.H., Wood, H., Ierullo, M., Majchrzak-Kita, B., Manguiat, K., Robinson, A., Kulasingam, V., Humar, A., and Kumar, D. (2022). Delayed-interval BNT162b2 mRNA COVID-19 vaccination enhances humoral immunity and induces robust T cell responses. Nat. Immunol. *23*, 380–385. https://doi.org/10.1038/s41590-021-01126-6.

11. Grunau, B., Goldfarb, D.M., Asamoah-Boaheng, M., Golding, L., Kirkham, T.L., Demers, P.A., and Lavoie, P.M. (2022). Immunogenicity of extended mRNA SARS-CoV-2 vaccine dosing intervals. JAMA *327*, 279–281. https://doi.org/10.1001/jama.2021.21921.

12. Payne, R.P., Longet, S., Austin, J.A., Skelly, D.T., Dejnirattisai, W., Adele, S., Meardon, N., Faustini, S., Al-Taei, S., Moore, S.C., et al. (2021). Immunogenicity of standard and extended dosing intervals of BNT162b2 mRNA vaccine. Cell *184*, 5699–5714.e11. https://doi.org/10.1016/j.cell.2021.10.011.

13. Tauzin, A., Gong, S.Y., Beaudoin-Bussières, G., Vézina, D., Gasser, R., Nault, L., Marchitto, L., Benlarbi, M., Chatterjee, D., Nayrac, M., et al. (2022). Strong humoral immune responses against SARS-CoV-2 Spike after BNT162b2 mRNA vaccination with a 16-week interval between doses. Cell Host Microbe *30*, 97–109.e5. https://doi.org/10.1016/j.chom.2021.12.004.

14. Gilbert, P.B., Montefiori, D.C., McDermott, A.B., Fong, Y., Benkeser, D., Deng, W., Zhou, H., Houchens, C.R., Martins, K., Jayashankar, L., et al. (2022). Immune correlates analysis of the mRNA-1273 COVID-19 vaccine efficacy clinical trial. Science *375*, 43–50.

15. Earle, K.A., Ambrosino, D.M., Fiore-Gartland, A., Goldblatt, D., Gilbert, P.B., Siber, G.R., Dull, P., and Plotkin, S.A. (2021). Evidence for antibody as a protective correlate for COVID-19 vaccines. Vaccine *39*, 4423–4428. https://doi.org/10.1016/j.vaccine.2021.05.063.

16. Crotty, S. (2019). T follicular helper cell biology: a decade of discovery and diseases. Immunity *50*, 1132–1148. https://doi.org/10.1016/j.immuni.2019.04.011.

17. Morita, R., Schmitt, N., Bentebibel, S.-E., Ranganathan, R., Bourdery, L., Zurawski, G., Foucat, E., Dullaers, M., Oh, S., Sabzghabaei, N., et al. (2011). Human blood CXCR5+CD4+ T cells are counterparts of T follicular cells and contain specific subsets that differentially support antibody secretion. Immunity *34*, 108–121. https://doi.org/10.1016/j.immuni.2010.12.012.

18. Kim, W., Zhou, J.Q., Horvath, S.C., Schmitz, A.J., Sturtz, A.J., Lei, T., Liu, Z., Kalaidina, E., Thapa, M., Alsoussi, W.B., et al. (2022). Germinal centre-driven maturation of B cell response to mRNA vaccination. Nature *604*, 141–145. https://doi.org/10.1038/s41586-022-04527-1.

19. Pardi, N., Hogan, M.J., Naradikian, M.S., Parkhouse, K., Cain, D.W., Jones, L., Moody, M.A., Verkerke, H.P., Myles, A., Willis, E., et al. (2018). Nucleoside-modified mRNA vaccines induce potent T follicular helper and germinal center B cell responses. J. Exp. Med. *215*, 1571–1588. https://doi.org/10.1084/jem.20171450.

20. Laidlaw, B.J., Craft, J.E., and Kaech, S.M. (2016). The multifaceted role of CD4(+) T cells in CD8(+) T cell memory. Nat. Rev. Immunol. *16*, 102–111. https://doi.org/10.1038/nri.2015.10.

21. Nayrac, M., Dubé, M., Sannier, G., Nicolas, A., Marchitto, L., Tastet, O., Tauzin, A., Brassard, N., Lima-Barbosa, R., Beaudoin-Bussières, G., et al. (2022). Temporal associations of B and T cell immunity with robust vaccine responsiveness in a 16-week interval BNT162b2 regimen. Cell Rep. *39*, 111013. https://doi.org/10.1016/j.celrep.2022.111013.

22. O'Shea, J.J., and Paul, W.E. (2010). Mechanisms underlying lineage commitment and plasticity of helper CD4+ T cells. Science *327*, 1098–1102. https://doi.org/10.1126/science.1178334.

23. Rodda, L.B., Morawski, P.A., Pruner, K.B., Fahning, M.L., Howard, C.A., Franko, N., Logue, J., Eggenberger, J., Stokes, C., Golez, I., et al. (2022). Imprinted SARS-CoV-2-specific memory lymphocytes define hybrid immunity. Cell *185*, 1588–1601.e14. https://doi.org/10.1016/j.cell.2022.03.018.

24. Painter, M.M., Mathew, D., Goel, R.R., Apostolidis, S.A., Pattekar, A., Kuthuru, O.,

Baxter, A.E., Herati, R.S., Oldridge, D.A., Gouma, S., et al. (2021). Rapid induction of antigen-specific CD4(+) T cells is associated with coordinated humoral and cellular immunity to SARS-CoV-2 mRNA vaccination. Immunity *54*, 2133–2142.e3. https://doi.org/10.1016/j.immuni.2021.08.001.

25. Goel, R.R., Painter, M.M., Apostolidis, S.A., Mathew, D., Meng, W., Rosenfeld, A.M., Lundgreen, K.A., Reynaldi, A., Khoury, D.S., Pattekar, A., et al. (2021). mRNA vaccines induce durable immune memory to SARS-CoV-2 and variants of concern. Science *374*, eabm0829. https://doi.org/10.1126/science.abm0829.

26. Zollner, A., Watschinger, C., Rössler, A., Farcet, M.R., Penner, A., Böhm, V., Kiechl, S.J., Stampfel, G., Hintenberger, R., Tilg, H., et al. (2021). B and T cell response to SARS-CoV-2 vaccination in health care professionals with and without previous COVID-19. EBioMedicine *70*, 103539. https://doi.org/10.1016/j.ebiom.2021.103539.

27. Flaxman, A., Marchevsky, N.G., Jenkin, D., Aboagye, J., Aley, P.K., Angus, B., Belij-Rammerstorfer, S., Bibi, S., Bittaye, M., Cappuccini, F., et al. (2021). Reactogenicity and immunogenicity after a late second dose or a third dose of ChAdOx1 nCoV-19 in the UK: a substudy of two randomised controlled trials (COV001 and COV002). Lancet *398*, 981–990. https://doi.org/10.1016/s0140-6736(21)01699-8.

28. Klumpp-Thomas, C., Kalish, H., Drew, M., Hunsberger, S., Snead, K., Fay, M.P., Mehalko, J., Shunmugavel, A., Wall, V., Frank, P., et al. (2021). Standardization of ELISA protocols for serosurveys of the SARS-CoV-2 pandemic using clinical and at-home blood sampling. Nat. Commun. *12*, 113. https://doi.org/10.1038/s41467-020-20383-x.

29. Hicks, J., Klumpp-Thomas, C., Kalish, H., Shunmugavel, A., Mehalko, J., Denson, J.P., Snead, K.R., Drew, M., Corbett, K.S., Graham, B.S., et al. (2021). Serologic cross-reactivity of SARS-CoV-2 with endemic and seasonal Betacoronaviruses. J. Clin. Immunol. *41*, 906–913. https://doi.org/10.1007/s10875-021-00997-6.

30. Anand, S.P., Prevost, J., Nayrac, M., Beaudoin-Bussieres, G., Benlarbi, M., Gasser, R., Brassard, N., Laumaea, A., Gong, S.Y., Bourassa, C., et al. (2021). Longitudinal analysis of humoral immunity against SARS-CoV-2 Spike in convalescent individuals up to 8 months post-symptom onset. Cell reports. Medicine *2*, 100290. https://doi.org/10.1016/j.xcrm.2021.100290.

31. Tangye, S.G., Liu, Y.J., Aversa, G., Phillips, J.H., and de Vries, J.E. (1998). Identification of functional human splenic memory B cells by expression of CD148 and CD27. J. Exp. Med. *188*, 1691–1703. https://doi.org/10.1084/jem.188.9.1691.

32. Moore, K.W., Rogers, J., Hunkapiller, T., Early, P., Nottenburg, C., Weissman, I., Bazin, H., Wall, R., and Hood, L.E. (1981). Expression of IgD may use both DNA rearrangement and RNA splicing mechanisms. Proc. Natl. Acad. Sci. USA *78*, 1800–1804. https://doi.org/10.1073/pnas.78.3.1800.

33. Niessl, J., Baxter, A.E., Mendoza, P., Jankovic, M., Cohen, Y.Z., Butler, A.L., Lu, C.L., Dubé, M., Shimeliovich, I., Gruell, H., et al. (2020). Combination anti-HIV-1 antibody therapy is associated with increased virus-specific T cell immunity. Nat. Med. *26*, 222–227. https://doi.org/10.1038/s41591-019-0747-1.

34. Patrick, D.M., Petric, M., Skowronski, D.M., Guasparini, R., Booth, T.F., Krajden, M., McGeer, P., Bastien, N., Gustafson, L., Dubord, J., et al. (2006). An outbreak of human Coronavirus OC43 infection and serological cross-reactivity with SARS Coronavirus. Can. J. Infect Dis. Med. Microbiol. *17*, 330–336. https://doi.org/10.1155/2006/152612.

35. Saib, I., Aleisa, S., Ardah, H., Mahmoud, E., Alharbi, A.O., Alsaedy, A., Aljohani, S., Alshehri, A., Alharbi, N.K., and Bosaeed, M. (2021). Non-SARS non-MERS human coronaviruses: clinical characteristics and outcome. Pathogens *10*, 1549. https://doi.org/10.3390/pathogens10121549.

36. Swadling, L., Diniz, M.O., Schmidt, N.M., Amin, O.E., Chandran, A., Shaw, E., Pade, C., Gibbons, J.M., Le Bert, N., Tan, A.T., et al. (2022). Pre-existing polymerase-specific T cells expand in abortive seronegative SARS-CoV-2. Nature *601*, 110–117. https://doi.org/10.1038/s41586-021-04186-8.

37. Morgan, X.C., Kabakchiev, B., Waldron, L., Tyler, A.D., Tickle, T.L., Milgrom, R., Stempak, J.M., Gevers, D., Xavier, R.J., Silverberg, M.S., and Huttenhower, C. (2015). Associations between host gene expression, the mucosal microbiome, and clinical outcome in the pelvic pouch of patients with inflammatory bowel disease. Genome Biol. *16*, 67. https://doi.org/10.1186/s13059-015-0637-x.

38. Day, C.E., Zhang, S.D., Riley, J., Gant, T., Wardlaw, A.J., and Guillen, C. (2009). A novel method for isolation of human lung T cells from lung resection tissue reveals increased expression of GAPDH and CXCR6. J. Immunol. Methods *342*, 91–97. https://doi.org/10.1016/j.jim.2008.12.001.

39. Quebec, G.o. (2022). COVID-19 Vaccination Guidelines. https://www.quebec.ca/en/health/advice-and-prevention/vaccination/covid-19-vaccine.

40. Chatterjee, D., Tauzin, A., Marchitto, L., Gong, S.Y., Boutin, M., Bourassa, C., Beaudoin-Bussières, G., Bo, Y., Ding, S., Laumaea, A., et al. (2022). SARS-CoV-2 Omicron Spike recognition by plasma from individuals receiving BNT162b2 mRNA vaccination with a 16-week interval between doses. Cell Rep. *38*, 110429. https://doi.org/10.1016/j.celrep.2022.110429.

41. Tauzin, A., Gong, S.Y., Painter, M.M., Goel, R.R., Chatterjee, D., Beaudoin-Bussières, G., Marchitto, L., Boutin, M., Laumaea, A., Okeny, J., et al. (2022). A boost with SARS-CoV-2 BNT162b2 mRNA vaccine elicits strong humoral responses independently of the interval between the first two doses. Preprint at medRxiv. https://doi.org/10.1101/2022.04.18.22273967.

42. Turner, J.S., O'Halloran, J.A., Kalaidina, E., Kim, W., Schmitz, A.J., Zhou, J.Q., Lei, T., Thapa, M., Chen, R.E., Case, J.B., et al. (2021). SARS-CoV-2 mRNA vaccines induce persistent human germinal centre responses. Nature *596*, 109–113. https://doi.org/10.1038/s41586-021-03738-2.

43. Cho, A., Muecksch, F., Schaefer-Babajew, D., Wang, Z., Finkin, S., Gaebler, C., Ramos, V., Cipolla, M., Mendoza, P., Agudelo, M., et al. (2021). Anti-SARS-CoV-2 receptor-binding domain antibody evolution after mRNA vaccination. Nature *600*, 517–522. https://doi.org/10.1038/s41586-021-04060-7.

44. Paschold, L., Klee, B., Gottschick, C., Willscher, E., Diexer, S., Schultheiß, C., Simnica, D., Sedding, D., Girndt, M., Gekle, M., et al. (2022). Rapid hypermutation B cell trajectory recruits previously primed B cells upon third SARS-Cov-2 mRNA vaccination. Front. Immunol. *13*, 876306. https://doi.org/10.3389/fimmu.2022.876306.

45. Jenks, S.A., Cashman, K.S., Zumaquero, E., Marigorta, U.M., Patel, A.V., Wang, X., Tomar, D., Woodruff, M.C., Simon, Z., Bugrovsky, R., et al. (2018). Distinct effector B cells induced by unregulated toll-like receptor 7 contribute to pathogenic responses in systemic lupus erythematosus. Immunity *49*, 725–739.e6. https://doi.org/10.1016/j.immuni.2018.08.015.

46. Wei, C., Anolik, J., Cappione, A., Zheng, B., Pugh-Bernard, A., Brooks, J., Lee, E.H., Milner, E.C.B., and Sanz, I. (2007). A new population of cells lacking expression of CD27 represents a notable component of the B cell memory compartment in systemic lupus erythematosus. J. Immunol. *178*, 6624–6633. https://doi.org/10.4049/jimmunol.178.10.6624.

47. Ruschil, C., Gabernet, G., Lepennetier, G., Heumos, S., Kaminski, M., Hracsko, Z., Irmler, M., Beckers, J., Ziemann, U., Nahnsen, S., et al. (2020). Specific induction of double negative B cells during protective and pathogenic immune responses. Front. Immunol. *11*, 606338. https://doi.org/10.3389/fimmu.2020.606338.

48. Shrock, E., Fujimura, E., Kula, T., Timms, R.T., Lee, I.H., Leng, Y., Robinson, M.L., Sie, B.M., Li, M.Z., Chen, Y., et al. (2020). Viral epitope profiling of COVID-19 patients reveals cross-reactivity and correlates of severity. Science *370*, eabd4250. https://doi.org/10.1126/science.abd4250.

49. Grifoni, A., Weiskopf, D., Ramirez, S.I., Mateus, J., Dan, J.M., Moderbacher, C.R., Rawlings, S.A., Sutherland, A., Premkumar, L., Jadi, R.S., et al. (2020). Targets of T Cell responses to SARS-CoV-2 Coronavirus in humans with COVID-19 disease and unexposed individuals. Cell *181*, 1489–1501.e15. https://doi.org/10.1016/j.cell.2020.05.015.

50. Mateus, J., Grifoni, A., Tarke, A., Sidney, J., Ramirez, S.I., Dan, J.M., Burger, Z.C., Rawlings, S.A., Smith, D.M., Phillips, E., et al. (2020). Selective and cross-reactive SARS-CoV-2 T cell epitopes in unexposed humans. Science *370*, 89–94. https://doi.org/10.1126/science.abd3871.

51. Braun, J., Loyal, L., Frentsch, M., Wendisch, D., Georg, P., Kurth, F., Hippenstiel, S., Dingeldey, M., Kruse, B., Fauchere, F., et al. (2020). SARS-CoV-2-reactive T cells in healthy donors and patients with COVID-19. Nature *587*, 270–274. https://doi.org/10.1038/s41586-020-2598-9.

52. Loyal, L., Braun, J., Henze, L., Kruse, B., Dingeldey, M., Reimer, U., Kern, F., Schwarz, T., Mangold, M., Unger, C., et al. (2021). Cross-reactive CD4(+) T cells enhance SARS-CoV-2 immune responses upon infection and vaccination. Science *374*, eabh1823. https://doi.org/10.1126/science.abh1823.

53. Le Bert, N., Tan, A.T., Kunasegaran, K., Tham, C.Y.L., Hafezi, M., Chia, A., Chng, M.H.Y., Lin, M., Tan, N., Linster, M., et al. (2020). SARS-CoV-2-specific T cell immunity in cases of COVID-19 and SARS, and uninfected controls. Nature *584*, 457–462. https://doi.org/10.1038/s41586-020-2550-z.

54. Kumar, R., and Burns, E.A. (2008). Age-related decline in immunity: implications for vaccine responsiveness. Expert Rev. Vaccines *7*, 467–479. https://doi.org/10.1586/14760584.7.4.467.

55. Müller, L., Andrée, M., Moskorz, W., Drexler, I., Walotka, L., Grothmann, R., Ptok, J., Hillebrandt, J., Ritchie, A., Rabl, D., et al. (2021). Age-dependent immune response to the biontech/pfizer BNT162b2 Coronavirus disease 2019 vaccination. Clin. Infect. Dis. *73*, 2065–2072. https://doi.org/10.1093/cid/ciab381.

56. Prévost, J., Gasser, R., Beaudoin-Bussières, G., Richard, J., Duerr, R., Laumaea, A., Anand, S.P., Goyette, G., Benlarbi, M., Ding, S., et al. (2020). Cross-sectional evaluation of humoral responses against SARS-CoV-2 spike. Cell Rep. Med. *1*, 100126. https://doi.org/10.1016/j.xcrm.2020.100126.

57. Beaudoin-Bussières, G., Laumaea, A., Anand, S.P., Prévost, J., Gasser, R., Goyette, G., Medjahed, H., Perreault, J., Tremblay, T., Lewin, A., et al. (2020). Decline of humoral responses against SARS-CoV-2 spike in convalescent individuals. mBio *11*, 02590-20. https://doi.org/10.1128/mBio.02590-20.

58. Niessl, J., Baxter, A.E., Morou, A., Brunet-Ratnasingham, E., Sannier, G., Gendron-Lepage, G., Richard, J., Delgado, G.G., Brassard, N., Turcotte, I., et al. (2020). Persistent expansion and Th1-like skewing of HIV-specific circulating T follicular helper cells during antiretroviral therapy. EBioMedicine *54*, 102727. https://doi.org/10.1016/j.ebiom.2020.102727.

59. Morou, A., Brunet-Ratnasingham, E., Dubé, M., Charlebois, R., Mercier, E., Darko, S., Brassard, N., Nganou-Makamdop, K., Arumugam, S., Gendron-Lepage, G., et al. (2019). Altered differentiation is central to HIV-specific CD4(+) T cell dysfunction in progressive disease. Nat. Immunol. *20*, 1059–1070. https://doi.org/10.1038/s41590-019-0418-x.

60. Reiss, S., Baxter, A.E., Cirelli, K.M., Dan, J.M., Morou, A., Daigneault, A., Brassard, N., Silvestri, G., Routy, J.P., Havenar-Daughton, C., et al. (2017). Comparative analysis of activation induced marker (AIM) assays for sensitive identification of antigen-specific CD4 T cells. PLoS One *12*, e0186998. https://doi.org/10.1371/journal.pone.0186998.

61. Roederer, M., Nozzi, J.L., and Nason, M.C. (2011). SPICE: exploration and analysis of post-cytometric complex multivariate datasets. Cytometry A. *79*, 167–174. https://doi.org/10.1002/cyto.a.21015.

62. Tauzin, A., Gendron-Lepage, G., Nayrac, M., Anand, S.P., Bourassa, C., Medjahed, H., Goyette, G., Dubé, M., Bazin, R., Kaufmann, D.E., and Finzi, A. (2022). Evolution of anti-RBD IgG avidity following SARS-CoV-2 infection. Viruses *14*, 532.

STAR★METHODS

KEY RESOURCES TABLE

REAGENT or RESOURCE	SOURCE	IDENTIFIER
Antibodies		
UCHT1 (BUV395) [Human anti-CD3]	BD Biosciences	Cat#563546; Lot: 9058566; RRID:AB_2744387
1B5 (BUV 395) [Human anti-CCR10]	BD Biosciences	Cat# 565322; Lot: 1198884 RRID:AB_2739181
IA6-2 (BUV 563) [Human anti-IgD]	BD Biosciences	Cat# 741394; Lot: 2048494 RRID:AB_2870889
MI15 (BUV 661) [Human anti-CD138]	BD Biosciences	Cat# 749873; Lot: 1140733 RRID:AB_2874113
UCH-B1 (BUV 737) [Human anti-IgM]	BD Biosciences	Cat# 748928; Lot: 1154015 RRID:AB_2873331
ML5 (BUV 805) [Human anti-CD24]	BD Biosciences	Cat# 742010; Lot: 1154017 RRID:AB_2871308
G18-145 (BV421) [Human anti-IgG]	BD Biosciences	Cat# 562581; Lot: 1033053 RRID:AB_2737665
SJ25C1 (BV650) [Human anti-CD19]	Biolegend	Cat# 363026; Lot: B328293 RRID:AB_2564255
2H7 (BV711) [Human anti-CD20]	BD Biosciences	Cat# 563126; Lot: 2032072 RRID:AB_2313579
B-LY4 (BV786) [Human anti-CD21]	BD Biosciences	Cat# 740969; Lot: 1167364 RRID:AB_2740594
G46-6 (BB700) [Human anti-HLADR]	BD Biosciences	Cat# 566480; Lot: 1053189 RRID:AB_2744477
IS11-8E10 (PE) [Human anti-IgA]	Miltenyi	Cat# 130-113-476; Lot: 5210405486 RRID:AB_2733861
M-T271 (APC-R700) [Human anti-CD27]	BD Biosciences	Cat# 565116; Lot: 0262146 RRID:AB_2739074
UCHT1 (BUV496) [Human anti-CD3]	BD Biosciences	Cat#612941; Lot:1022424; RRID:AB_2870222
L200 (BV711) [Human anti-CD4]	BD Biosciences	Cat#563913; Lot:03000025; RRID:AB_2738484
SK3 (BB630) [Human anti-CD4]	BD Biosciences	Cat#624294 CUSTOM; Lot:0289566
RPA-T8 (BV570) [Human anti-CD8]	Biolegend	Cat#301037; Lot:B281322; RRID:AB_10933259
M5E2 (BUV805) [Human anti-CD14]	BD Biosciences	Cat#612902; Lot:0262150; RRID:AB_2870189
M5E2 (BV480) [Human anti-CD14]	BD Biosciences	Cat#746304; Lot: 9133961; RRID:AB_2743629

(*Continued on next page*)

Continued

REAGENT or RESOURCE	SOURCE	IDENTIFIER
3G8 (BV650) [Human anti-CD16]	Biolegend	Cat#302042; Lot:B323847; RRID:AB_2563801
HIB19 (APC-eFluor780) [Human anti-CD19]	Thermo Fisher Scientific	Cat#47-0199; Lot:2145095; RRID:AB_1582231
HIB19 (BV480) [Human anti-CD19]	BD Biosciences	Cat#746457; Lot:1021649; RRID:AB_2743759
HIT2 (BB790) [Human anti-CD38]	BD Biosciences	Cat# 624296 CUSTOM; Lot: 9119974
HI100 (PerCP Cy5.5) [Human anti-CD45RA]	BD Biosciences	Cat#563429; Lot:8332746; RRID:AB_2738199
NCAM16.2 (BUV737) [Human anti-CD56]	BD Biosciences	Cat#564448; Lot:8288818; RRID:AB_2744432
FN50 (PerCP-eFluor710) [Human anti-CD69]	Thermo Fisher Scientific	Cat#46-0699-42; Lot:1920361; RRID:AB_2573694
FN50 (BV650) [Human anti-CD69]	Biolegend	Cat# 310934; Lot:B303462; RRID:AB_2563158
H4A3 (BV786) [Human anti-CD107A]	BD Biosciences	Cat#563869; Lot:8144866; RRID:AB_2738458
ACT35 (APC) [Human anti-CD134 (OX40)]	BD Biosciences	Cat#563473; Lot:1015537; RRID:AB_2738230
4B4-1 (PE-Dazzle 594) [Human anti-CD137 (4-1BB)]	Biolegend	Cat# 309826; Lot:B253152; RRID:AB_2566260
TRAP1 (BV421) [Human anti-CD154 (CD40L)]	BD Biosciences	Cat#563886; Lot:9037850; RRID:AB_2738466
TRAP1 (PE) [Human anti-CD154 (CD40L)]	BD Biosciences	Cat#555700; Lot:7086896; RRID:AB_396050
J25D4 (BV421) [Human anti-CD185 (CXCR5)]	Biolegend	Cat# 356920; Lot:B325837; RRID:AB_2562303
B27 (PECy7) [Human anti-IFN-γ]	BD Biosciences	Cat#557643; Lot:8256597; RRID:AB_396760
MQ1-17H12 (PE-Dazzle594) [Human anti-IL-2]	Biolegend	Cat#500344; Lot:B2261476; RRID:AB_2564091
JES3-9D7 (PE) [Human anti-IL-10]	BD Biosciences	Cat#554498; Lot:8198773; RRID:AB_395434
eBio64CAP17 (eFluor660) [Human anti-IL-17A]	Thermo Fisher Scientific	Cat#50-7179-42; Lot:2151998; RRID:AB_11149126
Mab11 (Alexa Fluor 488) [Human anti-TNF-α]	Biolegend	Cat#502915; Lot:B285221; RRID:AB_493121
LIVE/DEAD Fixable dead cell	Thermo Fisher Scientific	L34960
Mouse monoclonal anti-SARS-CoV-2 Spike (CR3022)	Dr M. Gordon Joyce	RRID: AB_2848080
Goat anti-Human IgG Fc Cross-absorbed Secondary Antibody, HRP	Invitrogen	Cat#31413; RRID: AB_429693
Alexa Fluor 647 AffiniPure Goat Anti-Human IgA + IgG + IgM (H+L)	Jackson ImmunoResearch	Cat#109-605-064; RRID: AB_2337886
Biological samples		
SARS-CoV-2 naïve donor blood samples	This paper	N/A
Chemicals, peptides, and recombinant proteins		
Dulbecco's Modified Eagle's medium (DMEM)	Wisent	Cat#319-005-CL
Roswell Park Memorial Institute (RPMI)	ThermoFischer Scientific	Cat#61870036
Penicillin/Streptomycin	VWR	Cat#450-201-EL
Fetal Bovine Serum (FBS)	VWR	Cat#97068-085
Bovine Serum Albumin	Sigma	Cat#A7638
PepMix™ SARS-CoV-2 (Spike Glycoprotein)	JPT	Cat#PM-WCPV-S-1
Staphylococcal Enterotoxin B (SEB)	Toxin technology	Cat#BT202
Phosphate Buffered Saline (PBS)	ThermoFischer Scientific	Cat#10010023
Tween 20	Sigma	Cat#P9416-100ML
Freestyle 293F expression medium	ThermoFischer Scientific	Cat#12338018
Formaldehyde 37%	ThermoFischer Scientific	Cat#F79-500
ExpiFectamine 293 transfection reagent	ThermoFischer Scientific	Cat#A14525
Westen Lightning Plus-ECL, Enhanced Chemoluminescence Substrate	Perkin Elmer Life Sciences	Cat#NEL105001EA
Experimental models: Cell lines		
HEK293T cells	ATCC	Cat#CRL-3216; RRID: CVCL_0063
FreeStyle 293F cells	ThermoFischer Scientific	Cat#R79007; RRID: CVCL_D603

(*Continued on next page*)

Continued

REAGENT or RESOURCE	SOURCE	IDENTIFIER
Recombinant DNA		
pCAGGS-OC43 Spike	Prévost et al.[56]	N/A
Software and algorithms		
Flow Jo v10.8.0	Flow Jo	https://www.flowjo.com
GraphPad Prism v8.4.1	GraphPad	https://www.graphpad.com
R studio v4.1.0	R studio	https://rstudio.com

RESOURCE AVAILABILITY

Lead contact

Further information and requests for resources and reagents should be directed to and will be fulfilled by the lead contact, Daniel E. Kaufmann (daniel.kaufmann@chuv.ch).

Materials availability

All unique reagents generated during this study are available from the lead contact upon a material transfer agreement (MTA).

Data and code availability

The published article includes all datasets generated and analyzed for this study. This paper does not report any original code. Further information and requests for resources and reagents should be directed to and will be fulfilled by the lead contact Author (daniel.kaufmann@chuv.ch).

EXPERIMENTAL MODEL AND SUBJECT DETAILS

Ethics statement

All work was conducted in accordance with the Declaration of Helsinki in terms of informed consent and approval by an appropriate institutional board. Blood samples were obtained from donors who consented to participate in this research project at CHUM (19.381). Individuals from the Philadelphia cohort were enrolled in the study with approval from the University of Pennsylvania Institutional Review Board (IRB# 844642). All participants were otherwise healthy and did not report any history of chronic health conditions.

Participants

No specific criteria such as number of patients (sample size), clinical or demographic were used for inclusion, beyond negative PCR confirmation for SARS-CoV-2 infection. The study was conducted in 26 SARS-CoV-2 naïve individuals with a long interval, and 12 with a short interval. All the information is summarized in Table 1.

PBMCs collection

PBMCs were isolated from blood samples by Ficoll density gradient centrifugation and cryopreserved in liquid nitrogen until use.

Plasma and antibodies

Plasma samples were collected, heat-inactivated for 1 hour at 56°C and stored at −80°C until ready to use in subsequent experiments. Plasma samples from uninfected donors collected before the pandemic were used as negative controls and used to calculate the seropositivity threshold in our ELISA assay. The RBD-specific monoclonal antibody CR3022 was used as a positive control in ELISA assays. Horseradish peroxidase (HRP)-conjugated Abs able to detect the Fc region of human IgG (Invitrogen) was used as secondary Abs to detect Ab binding in ELISA experiments. Alexa Fluor-647-conjugated goat anti-human Abs able to detect all Ig isotypes (anti-human IgM+IgG+IgA; Jackson ImmunoResearch Laboratories) were used as secondary Ab to detect plasma binding in flow cytometry experiments.

Cell lines

293T human embryonic kidney cells (obtained from ATCC) were maintained at 37°C under 5% CO_2 in Dulbecco's modified Eagle's medium (DMEM) (Wisent) containing 5% fetal bovine serum (FBS) (VWR) and 100 μg/ml of penicillin-streptomycin (Wisent).

METHOD DETAILS

Protein expression and purification

FreeStyle 293F cells (Thermo Fisher Scientific) were grown in FreeStyle 293F medium (Thermo Fisher Scientific) to a density of 1 x 10^6 cells/mL at 37°C with 8% CO_2 with regular agitation (150 rpm). Cells were transfected with a plasmid coding for SARS-CoV-2 S RBD using ExpiFectamine 293 transfection reagent, as directed by the manufacturer (Invitrogen).[56,57] One week later, cells were pelleted and discarded. Supernatants were filtered using a 0.22 μm filter (Thermo Fisher Scientific). The recombinant RBD proteins were purified by nickel affinity columns, as directed by the manufacturer (Thermo Fisher Scientific). The RBD preparations were dialyzed against phosphate-buffered saline (PBS) and stored in aliquots at −80°C until further use. To assess purity, recombinant proteins were loaded on SDS-PAGE gels and stained with Coomassie Blue.

SARS-CoV-2-specific B cells characterization

To detect SARS-CoV-2-specific B cells, we conjugated recombinant RBD proteins with Alexa Fluor 488 or Alexa Fluor 594 (Thermo Fisher Scientific) according to the manufacturer's protocol. 2 × 10^6 frozen PBMC from SARS-CoV-2 naïve donors were prepared in Falcon® 5ml-round bottom polystyrene tubes at a final concentration of 4 × 10^6 cells/mL in RPMI 1640 medium (GIBCO) supplemented with 10% of fetal bovine serum (Seradigm), Penicillin- Streptomycin (GIBCO) and HEPES (GIBCO). After a rest of 2h at 37°C and 5% CO_2, cells were stained using LIVE/DEAD Fixable Aqua dead cell (Thermo Fisher Scientific, Waltham, MA) in DPBS (GIBCO) at 4°C for 20min. The detection of SARS-CoV-2-antigen specific B cells was done by adding the RBD probes to the antibody cocktail listed in Table S1. Staining was performed at 4°C for 30min and cells were fixed using 2% paraformaldehyde at 4°C for 15min. Stained PBMC samples were acquired on Symphony cytometer (BD Biosciences) and analyzed using FlowJo v10.8.0 software. To avoid excessive noise in phenotyping analyses, we only included donors in whom we detected ≥5 RBD-specific B cells at every time point.

Activation-induced marker (AIM) assay

The AIM assay[9,33,58,59] was adapted for SARS-CoV-2 specific CD4 and CD8 T cells, as previously described.[9] PBMCs were thawed and rested for 3h in 96-well flat-bottom plates in RPMI 1640 supplemented with HEPES, penicillin and streptomycin and 10% FBS. PBMCs were then split in 3 conditions of 1.7×10^6 PBMCs each: i) stimulated with an S glycoprotein peptide pool (0.5 μg/ml per peptide, corresponding to the pool of 315 overlapping peptides (15-mers) spanning the complete amino acid sequence of the Spike glycoprotein (JPT), ii) stimulated with *Staphylococcus enterotoxin B* (SEB) (0.5 μg/ml) as positive control and iii) a condition containing the same DMSO concentration as the Spike peptide pool stimulation served as a negative control. Cells were stimulated for 15h at 37°C and 5% CO_2. CXCR3, CCR6, CXCR6 and CXCR5 antibodies were added in culture 15 min before stimulation. Cells were stained using LIVE/DEAD Fixable Aqua dead cell (Thermo Fisher Scientific, Waltham, MA) for 20 min at 4 C then surface markers (30 min, 4°C). Abs used are listed in Table S2. Cells were fixed using 2% paraformaldehyde for 15 min at 4 C before acquisition on Symphony cytometer (BD Biosciences). Analyses were performed using FlowJo v10.8.0 software. To minimize noise and increase specificity in the qualitative phenotypic analysis, we included only samples for which the spike-specific signal was at least 2 times over background with ≥5 positive events.[33,60,61]

Intracellular cytokine staining (ICS)

The ICS assay was adapted to study SARS-CoV-2-specific T cells, as previously described.[9] PBMCs were thawed and rested for 2 h in RPMI 1640 medium supplemented with 10% FBS, Penicillin-Streptomycin (Thermo Fisher Scientific, Waltham, MA) and HEPES (Thermo Fisher scientific, Waltham, MA). PBMCs were then split in 3 conditions of 1.7×10^6 PBMCs each: i) stimulated with an S glycoprotein peptide pool (0.5 μg/ml per peptide, corresponding to the pool of 315 overlapping peptides (15-mers) spanning the complete amino acid sequence of the Spike glycoprotein (JPT), ii) stimulated with *Staphylococcus enterotoxin B* (SEB) (0.5 μg/ml) as positive control and iii) a condition containing the same DMSO

concentration as the Spike peptide pool stimulation served as a negative control. Cell stimulation was carried out for 6h in the presence of mouse anti-human CD107a, Brefeldin A and monensin (BD Biosciences, San Jose, CA) at 37°C and 5% CO_2. Cells were stained using LIVE/DEAD Fixable Aqua dead cell (Thermo Fisher Scientific, Waltham, MA) for 20 min at 4°C and surface markers (30 min, 4°C), followed by intracellular detection of cytokines using the IC Fixation/Permeabilization kit (Thermo Fisher Scientific, Waltham, MA) according to the manufacturer's protocol before acquisition on a Symphony flow cytometer (BD Biosciences) and analysis using FlowJo v10.8.0 software. Abs used are listed in Table S3.

Characterization of effector functions among total cytokine$^+$ cells, defined by our ORgate strategy, was conducted on donors with $\geq$5 cytokine$^+$ cells that represented a two-fold increase over the unstimulated condition to avoid biased phenotyping. Given these criteria, only D2 could be analyzed.

Enzyme-linked immunosorbent assay (ELISA) and RBD avidity index

The SARS-CoV-2 WT RBD ELISA assay used was previously described.[56,57] Briefly, recombinant SARS-CoV-2 WT RBD proteins (2.5 μg/ml), or bovine serum albumin (BSA) (2.5 μg/ml) as a negative control, were prepared in PBS and were adsorbed to plates (MaxiSorp Nunc) overnight at 4°C. Coated wells were subsequently blocked with blocking buffer (Tris-buffered saline [TBS] containing 0.1% Tween20 and 2% BSA) for 1h at room temperature. Wells were then washed four times with washing buffer (Tris-buffered saline [TBS] containing 0.1% Tween20). CR3022 mAb (50 ng/ml) or a 1/500 dilution of plasma were prepared in a diluted solution of blocking buffer (0.1% BSA) and incubated with the RBD-coated wells for 90 minutes at room temperature. Plates were washed four times with washing buffer followed by incubation with secondary Abs (diluted in a diluted solution of blocking buffer (0.4% BSA)) for 1h at room temperature, followed by four washes. To calculate the RBD-avidity index, we performed in parallel a stringent ELISA, where the plates were washed with a chaotropic agent, 8M of urea, and added to the washing buffer. This assay was previously described.[62] HRP enzyme activity was determined after the addition of a 1:1 mix of Western Lightning oxidizing and luminol reagents (Perkin Elmer Life Sciences). Light emission was measured with a LB942 TriStar luminometer (Berthold Technologies). The signal obtained with BSA was subtracted for each plasma and was then normalized to the signal obtained with CR3022 present in each plate. The seropositivity threshold was established using the following formula: mean of pre-pandemic SARS-CoV-2 negative plasma + (3 standard deviations of the mean of pre-pandemic SARS-CoV-2 negative plasma).

Cell surface staining and flow cytometry analysis

The plasmid encoding the HCoV-OC43 Spike was previously reported.[56] 293T cells were co-transfected with a GFP expressor (pIRES2-GFP, Clontech) in combination with a plasmid encoding the full-length HCoV-OC43 Spike. 48h post-transfection, Spike-expressing cells were stained with plasma (1/250 dilution). AlexaFluor-647-conjugated goat anti-human IgM+IgG+IgA Abs (1/800 dilution) were used as secondary Abs. The percentage of transfected cells (GFP+ cells) was determined by gating the living cell population based on viability dye staining (Aqua Vivid, Invitrogen). Samples were acquired on a LSRII cytometer (BD Biosciences) and data analysis was performed using FlowJo v10.7.1 (Tree Star).

QUANTIFICATION AND STATISTICAL ANALYSIS

Statistical analysis

Symbols represent biologically independent samples of HCW from LI and SI cohorts. Lines connect data from the same donor. Thick lines represent median values. Differences in responses for the same patient before and after vaccination were performed using Wilcoxon matched pair tests. Differences in responses between individuals from LI and SI cohorts were measured by Mann-Whitney tests. Wilcoxon and Mann-Whitney tests were generated using GraphPad Prism version 8.4.3 (GraphPad, San Diego, CA).[23] p values <0.05 were considered significant. p values are indicated for each comparison assessed. For descriptive correlations, Spearman's R correlation coefficient was applied. Significant Spearman test results are indicated by stars (*: $p < 0.1$, **: $p < 0.05$, ***: $p < 0.001$). For graphical representation on a log scale (but not for statistical tests), null values were arbitrarily set at the minimum values for each assay.

Software scripts and visualization

Graphics and pie charts were generated using GraphPad PRISM version 8.4.3 and ggplot2 (v3.3.3) in R (v4.1.0).